Inorganic Chemistry

Article

pubs.acs.org/IC

Studies of Iron(III) Porphyrinates Containing Silanethiolate Ligands

Daniel J. Meininger, Jonathan D. Caranto, Hadi D. Arman, and Zachary J. Tonzetich*

Department of Chemistry, University of Texas at San Antonio (UTSA), San Antonio, Texas 78249, United States

Supporting Information

ABSTRACT: The chemistry of several iron(III) porphyrinates containing silanethiolate ligands is described. The complexes are prepared by protonolysis reactions of silanethiols with the iron(III) precursors, [Fe(OMe)(TPP)] and [Fe(OH)(H_2O)(TMP)] (TPP = dianion of *meso*-tetraphenylporphine; TMP = dianion of *meso*-tetramesitylporphine). Each of the compounds has been fully characterized in solution and the solid state. The stability of the silanethiolate complexes versus other iron(III) porphyrinate complexes containing sulfur-based ligands allows for an examination of their reactivity with several biologically relevant small molecules including H_2S, NO, and 1-methylimidazole. Electrochemically, the silanethiolate complexes display a quasi-reversible one-electron oxidation event at potentials higher than that observed for an analogous arenethiolate complex. The behavior of these complexes versus other sulfur-ligated iron(III) porphyrinates is discussed.

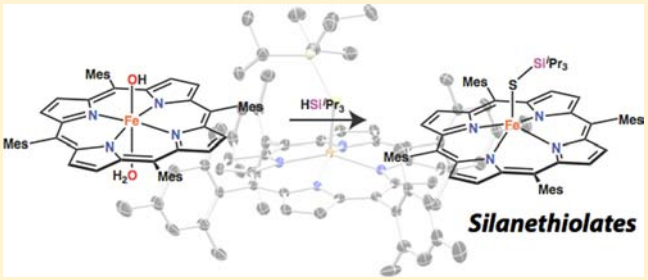

INTRODUCTION

The role of thiolate ligands in modulating the reactivity of biologically relevant transition metal ions has been well documented for a number of different ligand environments.[1] For heme-iron, the presence of cysteinate ligands in enzymes such as cytochrome P450 has been shown to modulate the reactivity of the metal cofactor in ways unique to that of other axially coordinated ligands.[2−8] In addition to thiols, the simplest of sulfhydryl containing species, hydrogen sulfide, has become of prominent interest due to its role in a variety of physiological processes in higher organisms.[9,10] Roles for H_2S in biology have now been demonstrated to include vasodilation,[11] signal transduction,[12] and protection against oxidative stress.[13] In addition, the potential for H_2S to serve as a source of elemental sulfur in the assembly of various cofactors makes the chemistry of this small molecule particularly intriguing. As a result, a great deal of recent work has centered on developing new platforms for detection of H_2S in vivo.[14−19]

The role of H_2S in biology begs the question of its molecular mechanisms of action. In this respect, parallels with the chemistry of other small signaling molecules such as NO and CO are notable.[20,21] Unlike these small molecules, however, the fundamental coordination chemistry of hydrogen sulfide at biologically relevant transition metal scaffolds has not been explored in detail.[22] This fact likely stems from a number of difficulties associated with H_2S including its toxicity, acidity, reducing potential, and propensity for forming intractable metal sulfides. In this vein, the porphyrin framework might be envisioned to provide a convenient platform for exploration of H_2S chemistry because its resistance to protonolysis coupled with its ability to constrain reactivity to mutually trans axial sites is beneficial in overcoming several of the challenges mentioned above. Furthermore, H_2S has been demonstrated to effect a variety of processes in heme proteins making basic understanding of this molecule in such environments important.[23−27]

Previous examinations of H_2S chemistry with metal porphyrinates have provided some key preliminary observations. With biological systems, the reaction of H_2S with hemoglobin and myoglobin to form "sulfhemes" has been known for over a century. These green reaction products originally observed by Hoppe-Seyler in 1866 were later shown to result predominantly from modification of the periphery of the porphyrin cofactor.[28−30] Bona fide binding of H_2S and HS^- to heme iron has also been reported,[31] most notably for the clam hemoglobin HbI from *Lucina pectinata*.[32−36] Despite this precedent, biological examples of hydrogen sulfide coordination remain scarce.

With synthetic porphyrin systems, work by Scheidt has demonstrated formation of hydrosulfide adducts of both iron(III)[37] and iron(II).[38] In related chemistry, Holm has reported a similar iron(III) hydrosulfide species as a transient intermediate in the reaction of $[Fe(OEP)]_2$-μ-O (OEP = dianion of octaethylporphine) with H_2S.[39] [Fe(SH)(OEP)] was proposed to be high-spin in line with other five-coordinate iron(III) thiolates containing porphyrinate ligands based on its NMR features.[40] More recently, H_2S binding to iron(II) was reported by Collman for a synthetic cyctochrome *c* model complex incorporating a picket fence type porphyrin ligand.[41,42]

In all these previous reports, the difficulty in preparing and isolating H_2S/HS^- species of iron porphyrinates has precluded detailed examinations of their reactivity and spectroscopy. Even in ruthenium chemistry, where binding of H_2S is well established,[43−49] examples involving porphyrinate ligands are

Received: June 10, 2013
Published: October 18, 2013

   dx.doi.org/10.1021/ic401467k | *Inorg. Chem.* 2013, 52, 12468−12476

Scheme 1

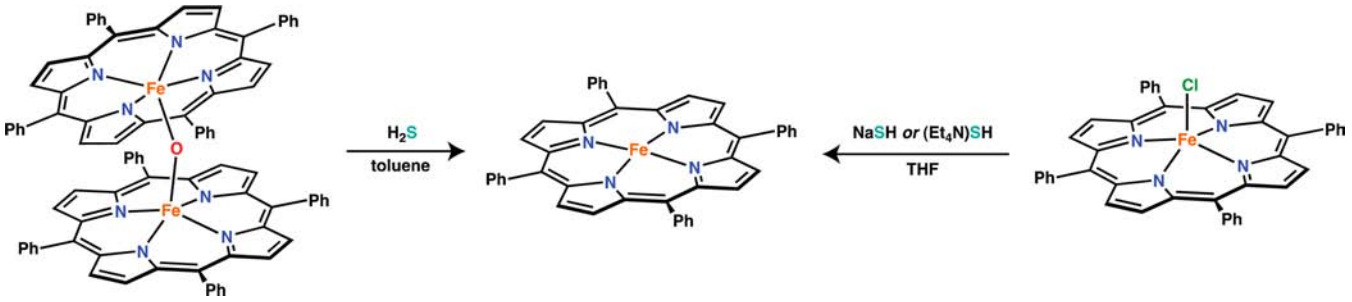

unknown. James has reported several thiol adducts of [Ru^{II}(TMP)] (TMP = *meso*-tetramesitylporphine), although analogous reactions with H_2S did not afford well-defined species.[50,51]

We have been examining the coordination chemistry of H_2S with transition metals in biologically relevant ligand scaffolds to elucidate the fundamental chemistry of such species relevant to the physiological action of hydrogen sulfide in biology. In this contribution, we describe our investigations of iron(III) porphyrinates with H_2S and silanethiols (R_3SiSH). The resulting silanethiolate complexes provide an alternative to hydrocarbyl−thiolates and appear to provide a stable platform for examining the chemistry of sulfur-bound iron(III) porphyrinates.

RESULTS AND DISCUSSION

Preparation and Characterization of Iron(III) Porphyrinates. Previous reports by Holm and Scheidt suggested the existence of the elusive iron(III) hydrosulfide complex, [Fe(SH)(P)] (P = porphyrinate ligand), although complete characterization and an examination of the reactivity of these species is lacking.[37,39] We therefore first examined the preparation of an analogous hydrosulfide iron(III) porphyrinate, [Fe(SH)(TPP)] (TPP = dianion of *meso*-tetraphenylporphine). Both protonolysis reactions of the oxo-bridged complex [Fe^{III}(TPP)]$_2$-μ-O with H_2S and salt metathesis reactions of [FeCl(TPP)] with NaSH or $(Et_4N)SH$ were examined in an attempt to prepare this species (Scheme 1). In each case, the iron(II) porphyrinate, [Fe^{II}(TPP)], was the only metal-containing species recovered from the reaction, consistent with previous observations by Holm.[39] For reactions employing hydrosulfide salts, we failed to observe formation of the previously reported hydrosulfide adduct of iron(II) under the conditions examined (1−3 equiv of HS$^-$).[38]

Replacement of TPP with the bulkier TMP ligand was examined in hopes of providing added stability to a putative hydrosulfide complex. Moreover, the TMP ligand allows for isolation of the terminal hydroxide complex, [Fe(OH)(H$_2$O)(TMP)], which we envisioned as a superior precursor to the oxo-bridged complex for protonolysis reactions employing sulfhydryls.[52] UV−vis spectroscopic observation of the reaction of [Fe(OH)(H$_2$O)(TMP)] with excess H_2S at room temperature did lead to formation of a new iron(III) complex (Figure 1), which we tentatively assigned as the desired [Fe(SH)(TMP)] complex on the basis of the position of the Soret absorbance and the *Q*-bands.[52] Repeating this reaction at the higher concentrations necessary for product isolation, however, resulted in formation of iron(II) as observed with the TPP ligand.

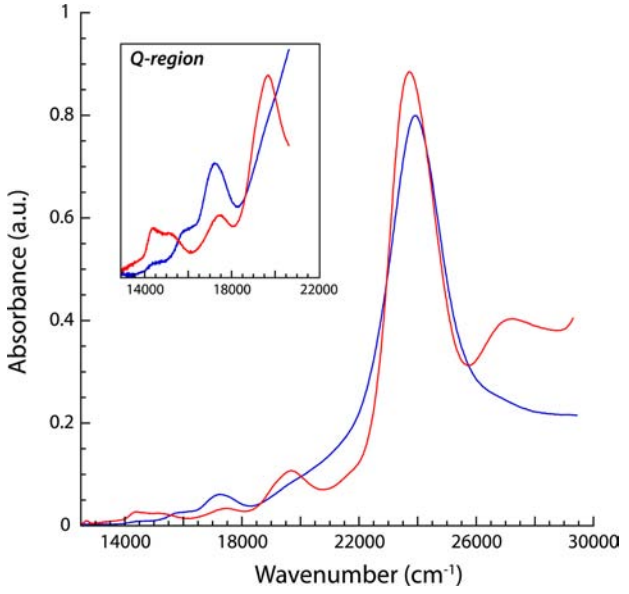

Figure 1. Electronic absorption spectra of 10 μM [Fe(OH)(TMP)] in toluene before (blue) and after (red) addition of excess H_2S at 23 °C. Inset displays a magnification of the *Q*-band region.

On the basis of the results obtained with H_2S and HS$^-$, we surmised that the propensity for reduction could be slowed by using an electronically similar ligand with greater steric bulk at sulfur. Select examples of five-coordinate iron(III) porphyrinates bearing thiolate ligands are known, all the structurally characterized examples of which contain arenethiolates.[40,53−62] Believing the hydrocarbon substituents of these thiolates to be poor models for the proton of the HS$^-$ ligand, we sought to examine the use of silanethiolates. The use of these ligands was also inspired in part by the analogy drawn between protons and trialkylsilyl groups in organic chemistry[63−65] and the noted stabilizing effect of silicon atoms alpha to anionic centers.[66,67] Furthermore, these ligands have been used as a source of sulfur equivalents previously,[39,68] offering the potential for deprotection to afford a hydrosulfide species.

To install the silanethiolate, we chose to examine protonolysis reactions akin to those described above for H_2S, reasoning that avoidance of thiolate salts would be beneficial in preventing the reduction to iron(II). Furthermore, such reactions are likely more relevant to the potential biological chemistry of sulfhydryls with iron heme centers containing Brønsted basic ligands such as hydroxide. We therefore examined reactions of the methoxide derivative, [Fe(OMe)(TPP)], with HSSi^{i}Pr$_3$ (hereafter HSTIPS) as shown in Scheme 2. This species was chosen because the corresponding iron(III) hydroxide complex is not stable for the TPP ligand.[69]

dx.doi.org/10.1021/ic401467k | Inorg. Chem. 2013, 52, 12468−12476

Scheme 2

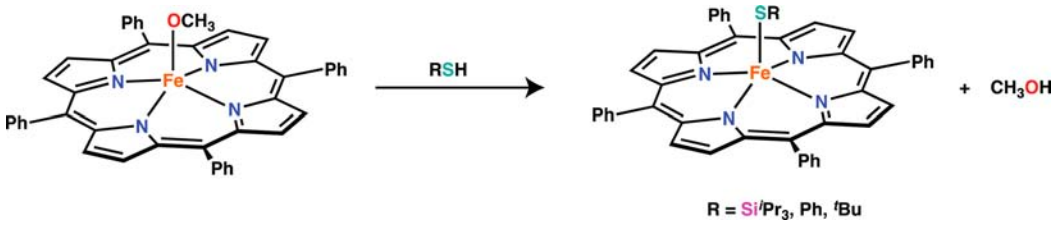

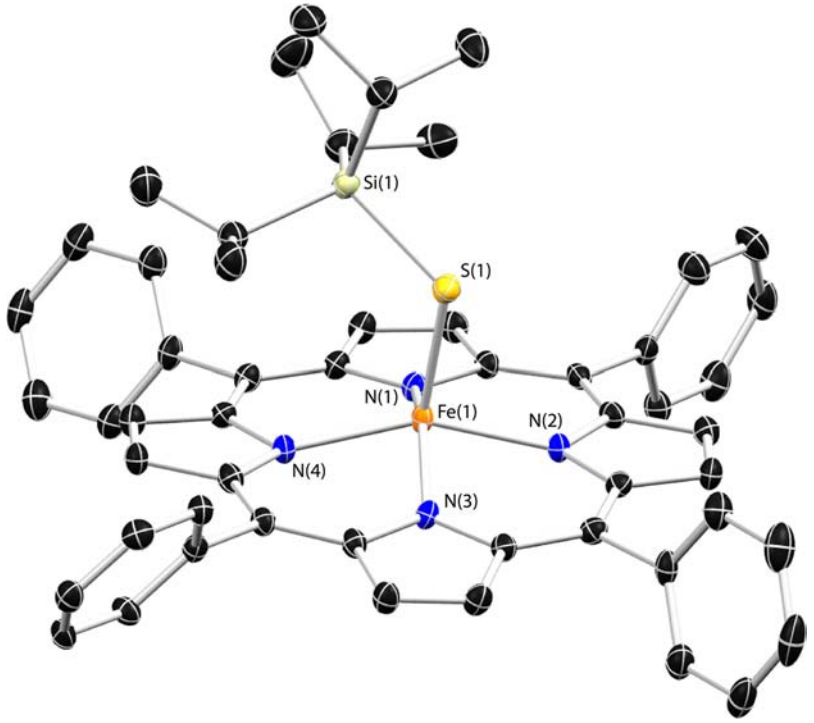

Figure 2. Thermal ellipsoid (50%) drawing of [Fe(STIPS)(TPP)]. Hydrogen atoms and cocrystallized benzene molecule omitted for clarity. Selected bond distances (Å) and angles (deg): Fe(1)−S(1) = 2.269(1); Fe(1)−N(1) = 2.082(2); Fe(1)−N(2) = 2.074(2); Fe(1)−N(3) = 2.088(2); Fe(1)−N(4) = 2.087(2); S(1)−Si(1) = 2.152(1); Fe(1)−S(1)−Si(1) = 115.78(4).

The reaction of HSTIPS with [Fe(OMe)(TPP)] proceeded rapidly in benzene or toluene, affording the iron(III) silanethiolate complex as a red solid in high yield. All preparations of [Fe(STIPS)(TPP)] also produced 5−10% of [Fe^{II}(TPP)] due to competing reduction. Similar reactions with PhSH and ^{t}BuSH also afforded the desired thiolate complexes as judged by ^{1}H NMR spectroscopy; however, in these instances, a larger degree of reduction was observed precluding isolation of these species (see Supporting Information).

The ^{1}H NMR features of [Fe(STIPS)(TPP)] are similar to those observed for other silanethiolate complexes of *meso*-substituted porphyrinates discussed below and are consistent with high-spin iron(III) complexes such as [FeCl(TPP)].[70] The pyrrolic protons of [Fe(STIPS)(TPP)] appear as a broad peak near 80 ppm in benzene-d_6. For all silanethiolate complexes investigated, this pyrrolic resonance is found 4−5 ppm downfield of that for the corresponding hydrocarbyl−thiolate complexes (cf. 76 ppm for [Fe(S^{t}Bu)(TPP)]). The meta hydrogen atoms of the phenyl substituents appear as two singlets at 12.31 and 11.00 ppm, the former of which overlaps a broad resonance at 12.7 ppm, which is most likely due to the isopropyl groups of the STIPS ligand (see Supporting Information).

The electronic absorption spectrum of [Fe(STIPS)(TPP)] in toluene displays a Soret feature centered at 24 000 cm^{-1} (417 nm), which appears to overlap several higher energy bands (see Supporting Information). The appearance of this Soret feature may be due to the presence of ∼5% [Fe^{II}(TPP)]; however, similar overlapping Soret features were observed for other silanethiolate species containing the TMP ligand (vida infra). The spectrum of [Fe(STIPS)(TPP)] also contains several less intense bands in the *Q* region, consistent with a five-coordinate iron(III) porphyrinate. These bands resemble those observed in the reaction of [Fe(OH)(H_2O)(TMP)] with H_2S described above, further supporting the assignment of the species in Figure 1 as the hydrosulfide iron(III) complex.

The solid-state structure of [Fe(STIPS)(TPP)] is depicted in Figure 2. The iron atom resides 0.561 Å out of the best-fit plane containing the porphyrin atoms and the Fe−S bond vector shows a deviation from the normal originating from the N_4 centroid as observed in other five-coordinate thiolate complexes.[61] The Fe−S bond distance of 2.269 Å is significantly below the range encountered for other structurally characterized [Fe^{III}(SR)(P)] species (cf. 2.32−2.36 Å),[71,72] highlighting the difference between the silanethiolate ligand and those based on hydrocarbyl-substituted thiols. Despite the

dx.doi.org/10.1021/ic401467k | *Inorg. Chem.* 2013, 52, 12468−12476

Scheme 3

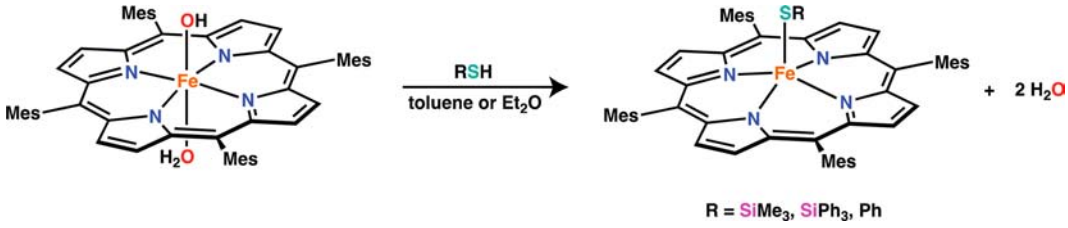

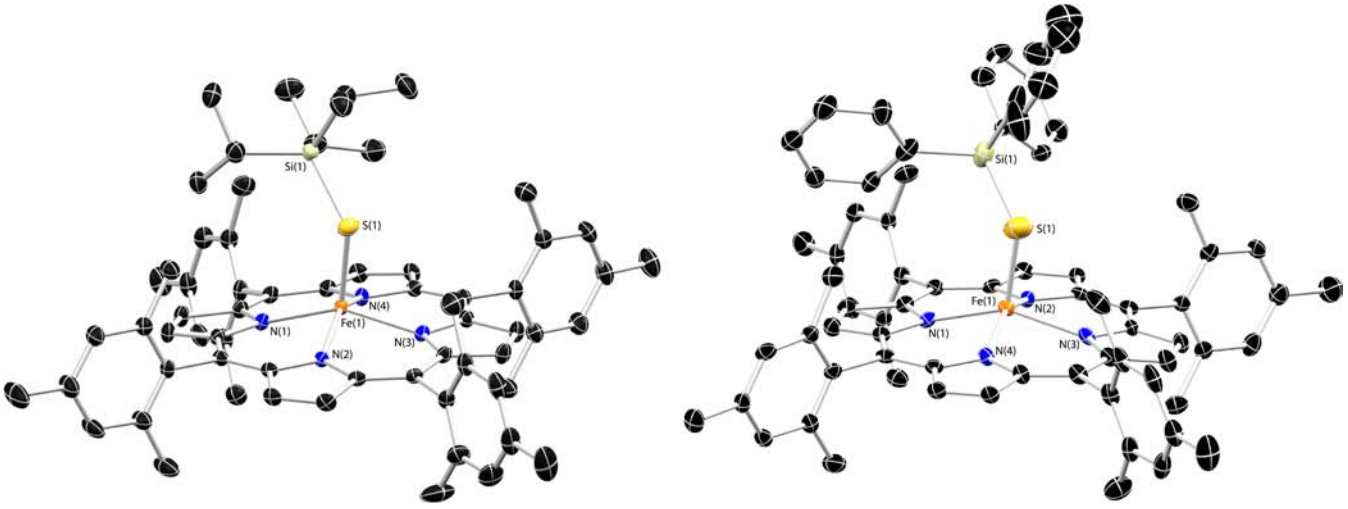

Figure 3. Thermal ellipsoid drawings of [Fe(STIPS)(TMP)] (50%) and [Fe(SSiPh$_3$)(TMP)] (35%). Hydrogen atoms and cocrystallized solvent molecules omitted for clarity. Selected bond distances (Å) and angles (deg). For [Fe(STIPS)(TMP)]: Fe(1)−S(1) = 2.273(1); Fe(1)−N(1) = 2.078(2); Fe(1)−N(2) = 2.080(2); Fe(1)−N(3) = 2.081(2); Fe(1)−N(4) = 2.081(2); S(1)−Si(1) = 2.134(1); Fe(1)−S(1)−Si(1) = 123.00(4). For [Fe(SSiPh$_3$)(TMP)]: Fe(1)−S(1) = 2.243(3); Fe(1)−N(1) = 2.062(5); Fe(1)−N(2) = 2.073(5); Fe(1)−N(3) = 2.090(6); Fe(1)−N(4) = 2.080(5); S(1)−Si(1) = 2.040(3); Fe(1)−S(1)−Si(1) = 127.1(2).

significant steric hindrance afforded by the Si^{i}Pr$_3$ group, the Fe−S−Si bond angle remains substantially bent at 115.78°.

Protonolysis reactions with the bulkier, more electron-rich TMP ligand were next examined with the intent of further stabilizing a trivalent silanethiolate complex and preventing reduction to iron(II). Reaction of [Fe(OH)(OH$_2$)(TMP)] with the silanethiols, HSTIPS and HSSiPh$_3$ afforded the corresponding thiolate species in good yield (Scheme 3). In contrast to similar reactions with TPP supported complexes, no reduction to iron(II) was observed with the TMP ligand. The benzenethiolate complex, [Fe(SPh)(TMP)], was also prepared by this route in sufficient purity to allow for isolation. Reactions with ^{t}BuSH afforded the *tert*-butanethiolate complex as judged by ^{1}H NMR spectroscopy. As with the TPP ligand, however, substantial reduction to [Fe^{II}(TMP)] was found to accompany the protonolysis reaction. Such a result is not surprising given the pronounced basicity of ^{t}BuS$^-$ with respect to PhS$^-$ and the silanethiolates. The ^{1}H NMR spectroscopic features of [Fe(STIPS)(TMP)] and [Fe(SSiPh$_3$)(TMP)] are similar to those of [Fe(STIPS)(TPP)] discussed above (see Supporting Information). Furthermore, the absorption spectra for all TMP complexes also resemble those of [Fe(STIPS)(TPP)], demonstrating a Soret feature that is complicated by the coincidence of other high energy absorptions (see Supporting Information).

The solid-state structures of [Fe(STIPS)(TMP)] and [Fe(SSiPh$_3$)(TMP)] are displayed in Figure 3 and show many similarities to the structure of [Fe(STIPS)(TPP)]. For the TMP complexes, the increased steric interactions between the silanethiolate ligand and the porphyrin *meso* substituents force the iron atom even farther out of the porphyrin plane (cf. 0.645 Å for [Fe(STIPS)(TMP)]). This effect is also observed for [Fe(SSiPh$_3$)(TMP)]; however, the metric parameters of this complex should be viewed cautiously as the structure refinement was problematic (R_1 = 9.0%). Crystals of [Fe(SPh)(TMP)] were also subjected to X-ray diffraction; however, the structure could not be refined satisfactorily (see Supporting Information). The diffraction data did establish the connectivity of the molecule unambiguously, displaying a similar positional disorder of the Fe−SPh moiety as found in the published structure of [Fe(SPh)(TPP)].[54]

To further establish the electronic structure of the silanethiolate complexes, EPR spectra of [Fe(STIPS)(TMP)] and [Fe(SSiPh$_3$)(TMP)] were recorded at 77 K in 2-MeTHF. Previous work has established that five-coordinate thiolate complexes of iron(III) porphyrinates adopt high-spin ground states displaying axial EPR signals with $g_\perp \approx 6$.[40,62,73] Such a result was confirmed for both [Fe(STIPS)(TMP)] and [Fe(SSiPh$_3$)(TMP)] in 2-MeTHF at 77 K (see Supporting Information). In contrast, the EPR spectrum of [Fe(SPh)(TMP)] in 2-MeTHF at 4 K displayed three signals. One of these signals corresponds to high-spin iron(III) and matches that observed for the silanethiolate complexes. The other two signals are consistent with a low-spin iron(III) thiolate.[74,75] Upon warming to 62 K, the high-spin signal decreases in intensity, suggesting that the appearance of the low-spin signals is not due to an impurity (see Supporting Information) but to an equilibrium between different spin states, possibly involving

dx.doi.org/10.1021/ic401467k | *Inorg. Chem.* 2013, 52, 12468−12476

solvent coordination.[76] The two low-spin signals display very similar g values and likely result from slightly different conformations of the complex in the frozen glass.

Electrochemistry. The electrochemistry of the silanethiolate complexes was next examined to understand their redox properties and help establish whether the propensity for reduction of iron(III) porphyrinates in reactions employing H_2S and other thiols is predominantly thermodynamic (high potential) or kinetic in origin. The CV for [Fe(STIPS)(TPP)] is displayed in Figure 4. A quasi-reversible one-electron

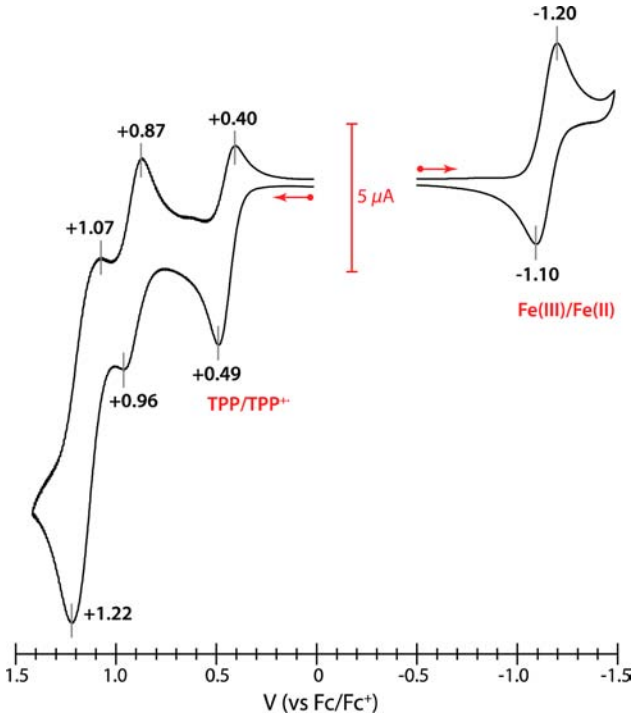

Figure 4. Cyclic voltammogram of 2 mM [Fe(STIPS)(TPP)] in CH_2Cl_2 at a Pt disk electrode. Scan rate is 50 mV/s, and the supporting electrolyte is 0.1 M Bu_4NPF_6.

reduction is found at a potential of $E_{1/2}$ = −1.15 V (versus Fc/Fc^+), suggesting that reduction to iron(II) is not very facile. The cyclic voltammograms of [Fe(STIPS)(TMP)] and [Fe(SSiPh$_3$)(TMP)] demonstrate cathodic events at similar potentials; although in each case, these events show a greatly attenuated return wave (see Supporting Information).

In the CV for all silanethiolate complexes examined, a quasi-reversible anode event is observed near +0.45 V. In the case of the Ph_3SiS^- complex, this event becomes nearly reversible at faster scan rates (see Supporting Information). The potentials found for these anode events are similar to those assigned as porphyrin-based oxidations ($P/P^{+\cdot}$) with other iron porphyrinates (cf. +0.61 V for [FeCl(TMP)]), however, they do not display the same degree of reversibility.[77] A possible explanation for this electrochemical behavior is that the oxidized iron(III) thiolate complexes contain considerable thiyl radical character. For comparison, the oxidation of free $^-$STIPS (as its Et_3NH^+ salt) under identical CV conditions occurs at a potential of +0.76 V (see Supporting Information). Partial dissociation of the thiyl radical on the electrochemical time scale would lead to the formation of disulfide and iron(III), accounting for the observed quasi-reversibility. Consistent with this proposal is the observation of peaks assignable to the iron(II)/iron(III) couple of [Fe(TPP)] in the return wave near −0.15 V (see Supporting Information). Such an explanation is also consistent with the proposal by Green that oxygenated cyctochrome P450 intermediates display sulfur localized ligand radical character.[78] Figure 5 shows the region of

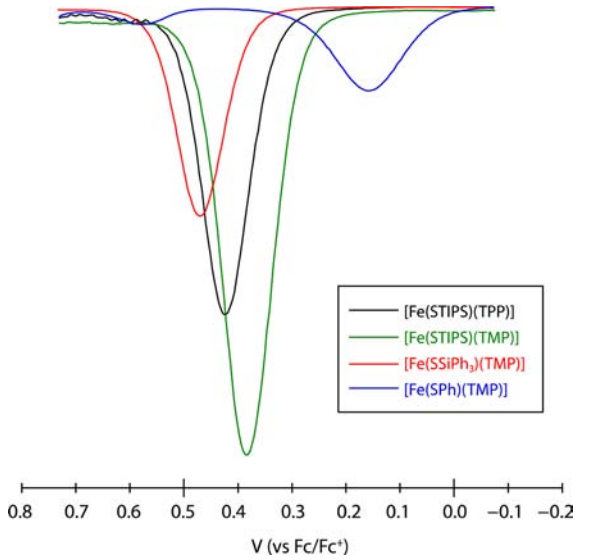

Figure 5. DPV of iron(III) thiolate complexes in CH_2Cl_2 at a Pt disk electrode highlighting the first observed oxidation event. Supporting electrolyte: 0.1 M Bu_4NPF_6.

the differential pulse voltammogram for all four thiolate species highlighting this first anodic event. Of interest is the fact that this oxidation event occurs at the lowest potential for the benzenethiolate complex despite the lower pK_a of PhSH versus trialkylsilanethiols.[79] This event is also completely irreversible for the benzenethiolate complex (see Supporting Information), again underscoring the unique features of the silanethiolates versus thiolates containing hydrocarbyl substituents.

In addition to the first quasi-reversible anode event discussed above, higher potential oxidation processes are observed for each of the thiolate complexes out to +1.3 V (see Supporting Information). Although we cannot assign these processes definitively at this time, the first of these high potential events coincides with the second of two reversible one-electron oxidation events displayed by other iron porphyrinate complexes.[80] In the case of [Fe(STIPS)(TPP)], this event is clearly resolved and nearly reversible ($E_{1/2}$ = +0.92 in Figure 4). In contrast to other iron porphyrinates, however, each of the thiolate complexes also displays an intense peak above +1.0 V that appears to correspond to a multielectron redox process ($E_{1/2}$ = +1.15 V in Figure 4). This multielectron event is not unique to the silanethiolate complexes and is also observed with the benzenethiolate species (see Supporting Information).

Reaction Chemistry. To probe the chemical behavior of the silanethiolate complexes, several reactions with biologically relevant molecules were investigated using the prototypical complex, [Fe(STIPS)(TMP)]. Treatment of the five-coordinate complex with 1-methylimidazole (1-MeIm) did not afford a six-coordinate thiolate species as judged by ^{1}H NMR spectroscopy but rather led to eventual reduction of iron(III) and isolation of [Fe(1-MeIm)$_2$(TMP)] (Scheme 4; see also Supporting Information).[81] A similar reduction was not observed in weakly coordinating solvents such as THF and 2-

dx.doi.org/10.1021/ic401467k | Inorg. Chem. 2013, 52, 12468−12476

Scheme 4

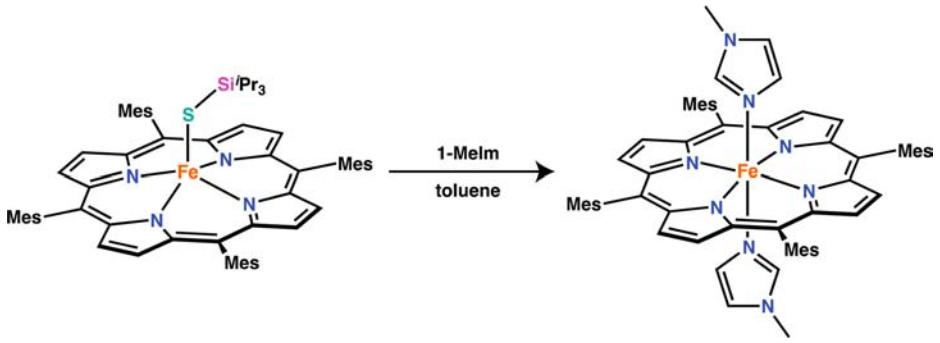

Scheme 5

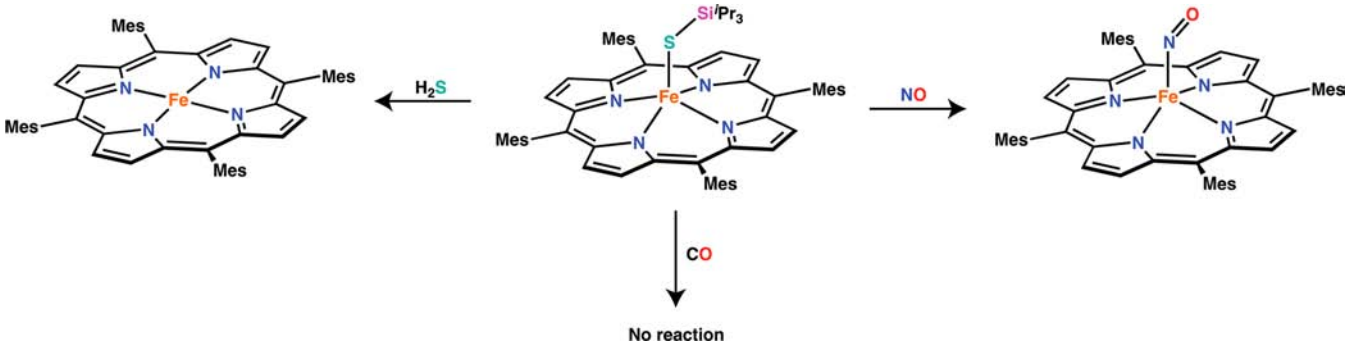

Scheme 6

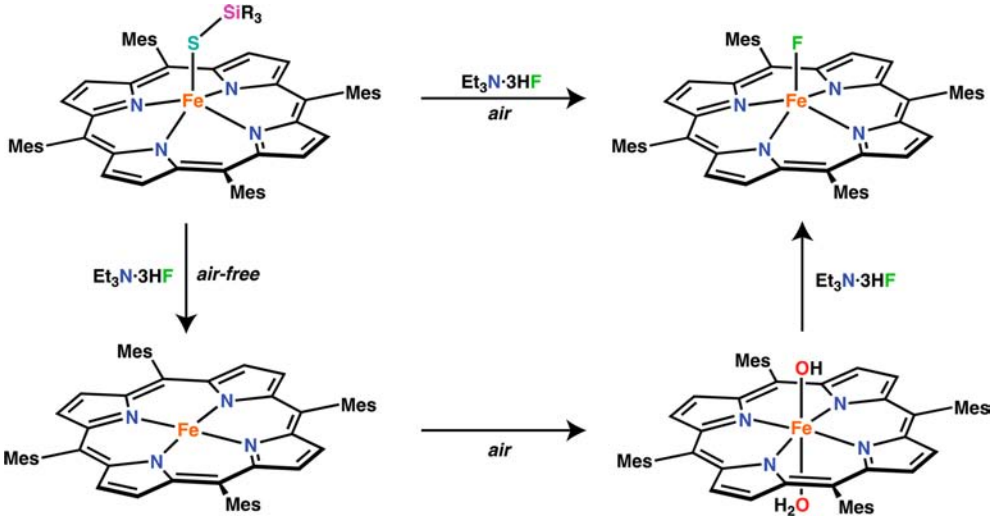

MeTHF (vida supra). This fact suggests that only strong Lewis bases are capable of binding to the silanethiolate complex, and that such coordination results in the reduction to iron(II).

Exposure of the iron(III) thiolate complexes to ambient atmosphere resulted in little to no decomposition as judged by NMR spectroscopy. Furthermore, the preparation of each of the thiolate complexes shown in Scheme 3 could be conducted in the presence of air with no decrease in reaction yield demonstrating their relative stability toward oxygen. Reaction of [Fe(STIPS)(TMP)] with other small molecules, however, was found to lead to different outcomes (Scheme 5). Introduction of 1 atm of CO(g) to a benzene-d_6 solution of [Fe(STIPS)(TMP)] resulted in no reaction after 24 h as judged by NMR spectroscopy. In contrast, introduction of 1 atm of NO(g) under identical conditions resulted in immediate formation of [Fe(NO)(TMP)], as judged by ^{1}H NMR, IR, and UV−vis spectroscopy (see Supporting Information).[82,83] The organic byproduct of this reaction is not known at this time but is presumably either the disulfide or the nitrosothiol, TIPSSNO. We favor the former based on similar findings by Richter-Addo.[61] The final gaseous small molecule examined was H_2S. Treatment of [Fe(STIPS)(TMP)] with 1 atm of H_2S in benzene-d_6 lead to immediate reduction and formation of [Fe^{II}(TMP)] in similar fashion to reactions starting from [Fe(OH)(H$_2$O)(TMP)].

In addition to biologically relevant small molecules, we also examined the reactivity of the silanethiolate complex with a fluoride source, Et$_3$N·3HF, anticipating that S−Si bond

dx.doi.org/10.1021/ic401467k | Inorg. Chem. 2013, 52, 12468−12476

Scheme 7

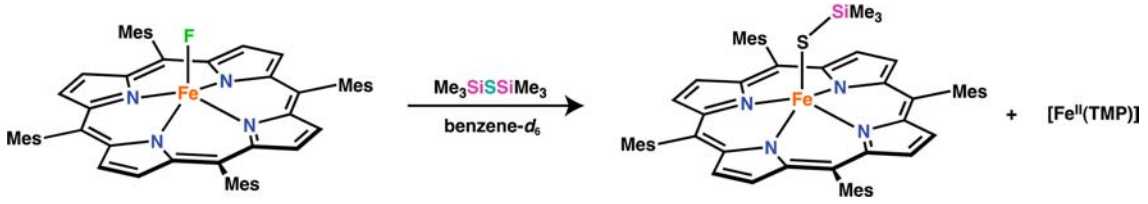

cleavage might represent another route to an iron(III) hydrosulfide complex. In the absence of oxygen, reaction of $Et_3N{\cdot}3HF$ with [Fe(STIPS)(TMP)] in benzene-d_6 afforded [Fe^{II}(TMP)] as judged by ^{1}H NMR spectroscopy. We could not identify a signal in the ^{19}F NMR spectrum of the reaction mixture corresponding to TIPSF and therefore do not know at this time whether the iron(II) porphyrinate is formed via the intermediacy of the desired iron(III) hydrosulfide or via a different pathway. Under ambient conditions, the iron(III) fluoride complex, [FeF(TMP)], can be isolated from the reaction mixture. Control experiments with [Fe(OH)(H_2O)-(TMP)] and $Et_3N{\cdot}3HF$ demonstrated formation of the same iron(III) fluoride complex consistent with previous work.[84] Thus, formation of [FeF(TMP)] in the presence of oxygen likely follows the reaction sequence shown in Scheme 6.

To assess the ability of [FeF(TMP)] to serve as a precursor to Fe−S bonds, the reaction shown in Scheme 7 was investigated. Upon treatment of [FeF(TMP)] with $(Me_3S)_2Si$ in benzene-d_6, a new iron(III) complex with *meta*-aryl resonances at 14.59 and 12.99 ppm was observed to form (see Supporting Information). We assigned this new species as [Fe(STMS)(TMP)] on the basis of the similarity of its NMR features to those compounds discussed above. Furthermore, the appearance of a resonance at −174 ppm in the ^{19}F NMR spectrum of the reaction mixture suggests that S−Si bond scission is occurring with concomitant formation of TMSF. Substantial [Fe^{II}(TPP)] was also observed to form under these conditions, demonstrating that the protonolysis route is a superior means of preparing silanethiolate ligated iron(III) porphyrinates.

CONCLUSIONS

We have reported the synthesis and characterization of several iron(III) porphyrinates containing silanethiolate ligands. The complexes are prepared by protonolysis reactions with the corresponding *O*-bound species representing a plausible reaction scenario for the interaction of sulfhydryls and iron(III) hemes in a biological setting. The presence of the silyl group on sulfur appears to give rise to notable differences in the structure and chemistry of these species compared with traditional iron(III) porphyrinates containing hydrocarbyl−thiolate ligands. The silanethiolate species are all high-spin and display five-coordinate geometries in the solid state with short Fe−S distances. Electrochemical measurements are consistent with a quasi-reversible initial oxidation event for each of the silanethiolate complexes, which contrasts with the completely irreversible event found for a related benzenethiolate complex. Finally, reaction pathways of the silanethiolate complexes with biologically relevant small molecules appear to be dominated by reduction to iron(II), including formation of a ferrous nitrosyl upon reaction with NO.

EXPERIMENTAL SECTION

General Comments. Unless otherwise noted, all manipulations were performed under an atmosphere of nitrogen gas using standard Schlenk technique or in a Vacuum Atmospheres glovebox under an atmosphere of purified nitrogen. Tetrahydrofuran, diethyl ether, methylene chloride, pentane, and toluene were purified by sparging with argon and passage through two columns packed with 4 Å molecular sieves. Benzene, benzene-d_6, and 2-methyltetrahydrofuan were dried over sodium then vacuum-distilled. All solvents were stored in the glovebox over 4 Å molecular sieves prior to use. ^{1}H NMR spectra were recorded in benzene-d_6 on a Varian INOVA spectrometer operating at 500 MHz and referenced to the residual C_6D_5H peak of the solvent (δ 7.16 ppm versus TMS). UV−vis spectra were recorded at ambient temperature in dichloromethane on a Cary-60 spectrophotometer in airtight Teflon-capped quartz cells. Cyclic voltammetry measurements were performed in dichloromethane in a single compartment cell under a nitrogen atmosphere (in the glovebox) at 25 °C using a CH Instruments 620D electrochemical workstation. A three-electrode setup was employed comprising a 1 mm diameter Pt disk working electrode, platinum wire auxiliary electrode, and Ag quasi-reference electrode. Triply recrystallized Bu_4NPF_6 was used as the supporting electrolyte. All electrochemical data were referenced internally to the ferrocene/ferrocenium couple at 0.00 V. EPR measurements were recorded in 4 mm quartz tubes on a Bruker E500 EPR spectrometer operating at the X-band at a modulation frequency of 100 kHz and modulation amplitude of 10 G. Low temperature measurements were made in frozen 2-MeTHF glasses at temperatures between 4 and 77 K with temperature control maintained by a helium (4−65 K) or nitrogen (77 K) flow cryostat (ESR900, Oxford Instruments, Inc.). Elemental analyses were performed by Atlantic Microlab, Inc. of Norcross, GA.

Materials. Metalloporphyrins [FeCl(TPP)], [Fe(OCH_3)(TPP)], [Fe^{III}(TPP)]-μ-O, [FeCl(TMP)], and [Fe(OH)(H_2O)(TMP)] were prepared by literature procedures or slight modifications thereof.[70,85−87] $Et_3N{\cdot}3HF$, ^{i}Pr_3SiSH, Ph_3SiSH, PhSH, and TMS_2S were purchased from Aldrich and used as received. NaSH was prepared by the method of Scheidt employing Na(s) and H_2S(g) in THF.[38] H_2S gas was purchased from Praxair and used as received. For experiments employing gaseous H_2S, the gas stream was delivered to the reaction vessel via a syringe needle interfaced to stainless steel tubing leading from the regulator. NO gas was purified by bubbling through 10 M NaOH(aq) then collected from the headspace of the solution.

X-ray Data Collection and Structure Solution Refinement. Crystals suitable for X-ray diffraction were mounted in Paratone oil onto a glass fiber and frozen under a nitrogen cold stream. The data were collected at 98(2) K using a Rigaku AFC12/Saturn 724 CCD fitted with Mo Kα radiation (λ = 0.710 73 Å). Data collection and unit cell refinement were performed using Crystal Clear software.[88] Data processing and absorption correction, giving minimum and maximum transmission factors, were accomplished with Crystal Clear and ABSCOR,[89] respectively. All structures were solved by direct methods and refined on F^2 using full-matrix, least-squares techniques with SHELXL-97.[90,91] All non-hydrogen atoms were refined with anisotropic displacement parameters. All carbon bound hydrogen atom positions were determined by geometry and refined by a riding model.

[Fe(SSi^{i}Pr$_3$)(TPP)]. To 50.0 mg (71.5 μmol) of [Fe(OCH_3)(TPP)] in 2 mL of toluene was added 12.5 μL (65.6 μmol) of ^{i}Pr_3SiSH. The solution color immediately changed from brown to red, and the

dx.doi.org/10.1021/ic401467k | Inorg. Chem. 2013, 52, 12468−12476

solution was allowed to stir at ambient temperature for 60 min. All volatiles were removed in vacuo, and the resulting residue was washed with pentane to afford 60.0 mg (98%) of a purple microcrystalline solid. NMR spectroscopy of bulk material showed the presence of methanol and ~5% [Fe^{II}(TPP)]. Crystals suitable for X-ray diffraction were grown by vapor diffusion of pentane into a saturated benzene solution at room temperature. ^{1}H NMR: δ 79.9 (v br s, pyr-*H*), 12.6 (v br s, TIPS), 12.31 (s, *m*-Ar*H*), 11.00 (*s*, *m*-Ar*H*), 7.9 (v br s, *o*-Ar*H*), 6.05 (s, *p*-Ar*H*), 4.8 (v br s, *o*-Ar*H*). UV−vis λ_{max}, cm^{-1} (ε, M^{-1} cm^{-1}): Soret 24 000 (87 000), *Q*-bands 19 600 (13 000), 17 600, 15 500, 14 600. Anal. Calcd for $C_{53}H_{49}FeN_4SSi{\cdot}CH_3OH$: C, 72.87; H, 6.00; N, 6.30. Found: C, 73.05; H, 5.78; N, 6.25.

[Fe(SSi^{i}Pr$_3$)(TMP)]. To 50.3 mg (57.6 μmol) of [Fe(OH)(H_2O)-(TMP)] in 3 mL of dissolved toluene was added 13 μL (68.2 μmol) of ^{i}Pr$_3$SiSH. The solution color immediately changed from brown-yellow to red, and the solution was allowed to stir at ambient temperature for 60 min. All volatiles were removed in vacuo, and the remaining residue was dissolved in 5 mL of pentane. The pentane solution was then evaporated to afford 56.6 mg (89%) of a dark purple microcrystalline solid. NMR spectroscopy of the bulk material from multiple syntheses showed the presence of pentane. Crystals suitable for X-ray diffraction were grown by slow cooling of a saturated pentane solution at −30 °C. ^{1}H NMR: δ 77.9 (v br s, pyr-*H*), 14.31 (s, *m*-Ar*H*), 12.92 (s, *m*-Ar*H*), 11.7 (v br s, TIPS), 7.0 (v br s, *o*-CH_3), 3.69 (s, *p*-CH_3), 2.5 (v br s, *o*-CH_3). UV−vis λ_{max}, cm^{-1} (ε, M^{-1} cm^{-1}): Soret 23 200 (62 000), *Q*-bands 19 500 (11 000), 17 500, 15 200, 14 500. Anal. Calcd for $C_{65}H_{73}FeN_4SSi{\cdot}C_5H_{12}$: C, 76.54; H, 7.80; N, 5.10. Found: C, 75.77; H, 7.69; N, 4.49.

[Fe(SSiPh$_3$)(TMP)]. To 50.2 mg (57.6 μmol) of [Fe(OH)(H_2O)-(TMP)] in 9 mL of dissolved toluene was added 16.8 mg (57.4 μmol) of Ph_3SiSH. The solution color immediately changed from brown-yellow to red, and the solution was allowed to stir at ambient temperature for 60 min. All volatiles were removed in vacuo, and the remaining residue was washed with pentane to afford 63.7 mg (98%) of a dark purple microcrystalline solid. Crystals suitable for X-ray diffraction were grown by vapor diffusion of pentane into a saturated dichloromethane solution of the complex. ^{1}H NMR: δ 78.4 (v br s, pyr-*H*), 15.09 (s, *m*-Ar*H*), 14.6 (br s, $SiPh_3$), 13.56 (s, *m*-Ar*H*), 7.0 (v br s, *o*-CH_3), 3.78 (s, *p*-CH_3), 3.2 (br, $SiPh_3$), 2.9 (v br s, *o*-CH_3). UV−vis λ_{max}, cm^{-1} (ε, M^{-1} cm^{-1}): Soret 23 900 (92 000), *Q*-bands 19 400 (17 000), 17 300, 14 900, 14 200. Anal. Calcd for $C_{74}H_{67}FeN_4SSi$: C, 78.77; H, 5.99; N, 4.97. Found: C, 78.69; H, 6.19; N, 4.60.

[Fe(SPh)(TMP)]. To 50.3 mg (57.6 μmol) of [Fe(OH)(H_2O)-(TMP)] in 3 mL of toluene was added 5.7 μL (51.7 μmol) of benzenethiol. The solution colored changed from brown-yellow to red, and the solution was allowed to stir at ambient temperature for 60 min. All volatiles were removed in vacuo, and the remaining residue was dissolved in 5 mL of pentane. The pentane solution was then evaporated to afford 55.7 mg (97%) of a dark purple microcrystalline solid. NMR spectroscopy of bulk material from multiple syntheses showed the presence of variable amounts of water. ^{1}H NMR: δ 73.9 (v br s, pyr-*H*), 70.4 (v br s, SPh), 13.97 (s, *m*-Ar*H*), 12.63 (*m*-Ar*H*), 6.3 (v br s, *o*-CH_3), 3.75 (s, *p*-CH_3), 3.2 (br s, SPh), 3.0 (v br s, *o*-CH_3). UV−vis λ_{max}, cm^{-1} (ε, M^{-1} cm^{-1}): Soret 24 300 (98 000), *Q*-bands 19 500 (17 000), 17 500, 14 700, 14 300. Anal. Calcd for $C_{62}H_{57}FeN_4S{\cdot}(H_2O)_{1.5}$: C, 76.53; H, 6.21; N, 5.76. Found: C, 76.51; H, 6.93, N, 4.81.

Procedure for NMR Scale Reactions with [Fe(STIPS)(TMP)]. To a septum-capped NMR tube containing a ~10 mM solution of [Fe(STIPS)(TMP)] in benzene-d_6 was introduced an excess of gaseous reagent (H_2S, NO, or CO). In the case of reactions employing 1-MeIm, $Et_3N{\cdot}3HF$, or $(Me_3Si)_2S$, a stoichiometric amount of the corresponding reagent was added as a neat liquid via microsyringe. Solutions were immediately subjected to ^{1}H NMR spectroscopy. For the reaction with NO(g), the solution was evaporated to dryness, and the remaining solid was used for IR spectroscopy (KBr). Crystals of [Fe(1-MeIm)$_2$(TMP)] were grown by layering of a benzene solution of the complex with pentane at room temperature.

■ ASSOCIATED CONTENT

Ⓢ Supporting Information

Additional spectra, thermal ellipsoid drawings for [Fe(SPh)-(TMP)] and [Fe(1-MeIm)$_2$(TMP)], cyclic voltammograms, crystallographic data, and refinement parameters for all complexes and the corresponding CIF files. This material is available free of charge via the Internet at http://pubs.acs.org.

■ AUTHOR INFORMATION

Notes

The authors declare no competing financial interest.

■ ACKNOWLEDGMENTS

This work was supported by a grant from the Welch Foundation (AX-1772 to Z.J.T.). J.D.C. is supported through the MBRS/RISE program (GM060655). The authors also acknowledge Mr. Salvador Echeveste, Jr. for experimental assistance through the support of the ACS Project SEED program.

■ REFERENCES

(1) Holm, R. H.; Kennepohl, P.; Solomon, E. I. *Chem. Rev.* **1996**, *96*, 2239−2314.
(2) Dawson, J. H.; Holm, R. H.; Trudell, J. R.; Barth, G.; Linder, R. E.; Bunnenberg, E.; Djerassi, C.; Tang, S. C. *J. Am. Chem. Soc.* **1976**, *98*, 3707−3709.
(3) Dawson, J. H.; Sono, M. *Chem. Rev.* **1987**, *87*, 1255−1276.
(4) Ogliaro, F.; de Visser, S. P.; Shaik, S. *J. Inorg. Biochem.* **2002**, *91*, 554−567.
(5) Meunier, B.; de Visser, S. l. P.; Shaik, S. *Chem. Rev.* **2004**, *104*, 3947−3980.
(6) Shaik, S.; Kumar, D.; de Visser, S. l. P.; Altun, A.; Thiel, W. *Chem. Rev.* **2005**, *105*, 2279−2328.
(7) Shaik, S.; Cohen, S.; Wang, Y.; Chen, H.; Kumar, D.; Thiel, W. *Chem. Rev.* **2009**, *110*, 949−1017.
(8) de Visser, S. P.; Nam, W. In *Handbook of Porphyrin Science*; World Scientific Publishing Co. Pte. Ltd.: Singapore, 2010; Vol. *10*, pp 85−139.
(9) Li, L.; Rose, P.; Moore, P. K. *Annu. Rev. Pharmacol. Toxicol.* **2011**, *51*, 169−187.
(10) Czyzewski, B. K.; Wang, D.-N. *Nature* **2012**, *483*, 494−497.
(11) Yang, G.; Wu, L.; Jiang, B.; Yang, W.; Qi, J.; Cao, K.; Meng, Q.; Mustafa, A. K.; Mu, W.; Zhang, S.; Snyder, S. H.; Wang, R. *Science* **2008**, *322*, 587−590.
(12) Olson, K. R. *Antioxid. Redox Signaling* **2012**, *17*, 32−44.
(13) Shatalin, K.; Shatalina, E.; Mironov, A.; Nudler, E. *Science* **2011**, *334*, 986−990.
(14) Lippert, A. R.; New, E. J.; Chang, C. J. *J. Am. Chem. Soc.* **2011**, *133*, 10078−10080.
(15) Qian, Y.; Karpus, J.; Kabil, O.; Zhang, S.-Y.; Zhu, H.-L.; Banerjee, R.; Zhao, J.; He, C. *Nat. Commun.* **2011**, *2*, 495.
(16) Chan, J.; Dodani, S. C.; Chang, C. J. *Nat. Chem.* **2012**, *4*, 973−984.
(17) Galardon, E.; Roger, T.; Deschamps, P.; Roussel, P.; Tomas, A.; Artaud, I. *Inorg. Chem.* **2012**, *51*, 10068−10070.
(18) Montoya, L. A.; Pluth, M. D. *Chem. Commun.* **2012**, *48*, 4767−4769.
(19) Lin, V. S.; Chang, C. J. *Curr. Opin. Chem. Biol.* **2012**, *16*, 595−601.
(20) Wang, R. *FASEB J.* **2002**, *16*, 1792−1798.
(21) Kajimura, M.; Fukuda, R.; Bateman, R. M.; Yamamoto, T.; Suematsu, M. *Antioxid. Redox Signal.* **2010**, *13*, 157−192.
(22) James, B. R. *Pure Appl. Chem.* **1997**, *69*, 2213−2220.
(23) Nicholls, P.; Kim, J. K. *Biochim. Biophys. Acta, Bioenerg.* **1981**, *637*, 312−320.
(24) Nicholls, P.; Kim, J. K. *Can. J. Biochem.* **1982**, *60*, 613−623.

(25) Hill, B. C.; Woon, T. C.; Nicholls, P.; Peterson, J.; Greenwood, C.; Thomson, A. J. *Biochem. J.* **1984**, *224*, 591−600.
(26) Blackstone, E.; Morrison, M.; Roth, M. B. *Science* **2005**, *308*, 518−518.
(27) Pietri, R.; Roman-Morales, E.; Lopez-Garriga, J. *Antiox. Redox Signal.* **2011**, *15*, 393−404.
(28) Johnson, E. A. *Biochim. Biophys. Acta, Protein Struct.* **1970**, *207*, 30−40.
(29) Berzofsky, J. A.; Peisach, J.; Blumberg, W. E. *J. Biol. Chem.* **1971**, *246*, 3367−3377.
(30) Berzofsky, J. A.; Peisach, J.; Horecker, B. L. *J. Biol. Chem.* **1972**, *247*, 3783−3791.
(31) Strianese, M.; De Martino, F.; Pellecchia, C.; Ruggiero, G.; D'Auria, S. *Protein Pept. Lett.* **2011**, *18*, 282−286.
(32) Kraus, D. W.; Wittenberg, J. B. *J. Biol. Chem.* **1990**, *265*, 16043−16053.
(33) Kraus, D. W.; Wittenberg, J. B.; Lu, J. F.; Peisach, J. *J. Biol. Chem.* **1990**, *265*, 16054−16059.
(34) Cerda-Colón, J. F.; Silfa, E.; López-Garriga, J. *J. Am. Chem. Soc.* **1998**, *120*, 9312−9317.
(35) Pietri, R.; Lewis, A.; León, R. G.; Casabona, G.; Kiger, L.; Yeh, S.-R.; Fernandez-Alberti, S.; Marden, M. C.; Cadilla, C. L.; López-Garriga, J. *Biochemistry* **2009**, *48*, 4881−4894.
(36) Román-Morales, E.; Pietri, R.; Ramos-Santana, B.; Vinogradov, S. N.; Lewis-Ballester, A.; López-Garriga, J. *Biochem. Biophys. Res. Commun.* **2010**, *400*, 489−492.
(37) English, D. R.; Hendrickson, D. N.; Suslick, K. S.; Eigenbrot, C. W.; Scheidt, W. R. *J. Am. Chem. Soc.* **1984**, *106*, 7258−7259.
(38) Pavlik, J. W.; Noll, B. C.; Oliver, A. G.; Schulz, C. E.; Scheidt, W. R. *Inorg. Chem.* **2010**, *49*, 1017−1026.
(39) Cai, L.; Holm, R. H. *J. Am. Chem. Soc.* **1994**, *116*, 7177−7188.
(40) Tang, S. C.; Koch, S.; Papaefthymiou, G. C.; Foner, S.; Frankel, R. B.; Ibers, J. A.; Holm, R. H. *J. Am. Chem. Soc.* **1976**, *98*, 2414−2434.
(41) Collman, J. P.; Ghosh, S.; Dey, A.; Decréau, R. A. *Proc. Natl. Acad. Sci. U. S. A.* **2009**, *106*, 22090−22095.
(42) Collman, J. P.; Ghosh, S. *Inorg. Chem.* **2010**, *49*, 5798−5810.
(43) Kuehn, C. C.; Taube, H. *J. Am. Chem. Soc.* **1976**, *98*, 689−702.
(44) Sellman, D.; Lechner, P.; Knoch, F.; Moll, M. *Angew. Chem., Int. Ed.* **1991**, *30*, 552−553.
(45) Ma, E. S. F.; Rettig, S. J.; James, B. R. *Chem. Commun.* **1999**, 2463−2464.
(46) Jessop, P. G.; Lee, C. L.; Rastar, G.; James, B. R.; Lock, C. J. L.; Faggiani, R. *Inorg. Chem.* **2002**, *31*, 4601−4605.
(47) Chatwin, S. L.; Diggle, R. A.; Jazzar, R. F. R.; Macgregor, S. A.; Mahon, M. F.; Whittlesey, M. K. *Inorg. Chem.* **2003**, *42*, 7695−7697.
(48) Ma, E. S. F.; Rettig, S. J.; Patrick, B. O.; James, B. R. *Inorg. Chem.* **2012**, *51*, 5427−5434.
(49) Galardon, E.; Daguet, H.; Deschamps, P.; Roussel, P.; Tomas, A.; Artaud, I. *Dalton Trans.* **2013**, *42*, 2817−2821.
(50) Rebouças, J. S.; Patrick, B. O.; James, B. R. *J. Am. Chem. Soc.* **2012**, *134*, 3555−3570.
(51) Rebouças, J. S.; James, B. R. *Inorg. Chem.* **2013**, *52*, 1084−1098.
(52) Brewer, C. *J. Chem. Soc., Chem. Commun.* **1990**, 344−346.
(53) Koch, S.; Tang, S. C.; Holm, R. H.; Frankel, R. B.; Ibers, J. A. *J. Am. Chem. Soc.* **1975**, *97*, 916−918.
(54) Collman, J. P.; Sorrell, T. N.; Hodgson, K. O.; Kulshrestha, A. K.; Strouse, C. E. *J. Am. Chem. Soc.* **1977**, *99*, 5180−5181.
(55) Miller, K. M.; Strouse, C. E. *Acta Crystallogr., Sect. C: Cryst. Struct. Commun.* **1984**, *40*, 1324−1327.
(56) Nasri, H.; Haller, K. J.; Wang, Y.; Huynh Boi, H.; Scheidt, W. R. *Inorg. Chem.* **1992**, *31*, 3459−3467.
(57) Ueyama, N.; Nishikawa, N.; Yamada, Y.; Okamura, T.-A.; Nakamura, A. *Inorg. Chim. Acta* **1998**, *283*, 91−97.
(58) Ueyama, N.; Nishikawa, N.; Yamada, Y.; Okamura, T.-A.; Oka, S.; Sakurai, H.; Nakamura, A. *Inorg. Chem.* **1998**, *37*, 2415−2421.
(59) Sun, W.-Y.; Zhang, L.; Gu, Q. *J. Electroanal. Chem.* **1999**, *469*, 84−87.
(60) Tani, F.; Matsu-ura, M.; Nakayama, S.; Naruta, Y. *Coord. Chem. Rev.* **2002**, *226*, 219−226.
(61) Xu, N.; Powell, D. R.; Cheng, L.; Richter-Addo, G. B. *Chem. Commun.* **2006**, *0*, 2030−2032.
(62) Das, P. K.; Chatterjee, S.; Samanta, S.; Dey, A. *Inorg. Chem.* **2012**, *51*, 10704−10714.
(63) Fleming, I. *Chem. Soc. Rev.* **1981**, *10*, 83−111.
(64) Hwu, J. R.; Wetzel, J. M. *J. Org. Chem.* **1985**, *50*, 3946−3948.
(65) Hwu, J. R.; Wang, N. *Chem. Rev.* **1989**, *89*, 1599−1615.
(66) Brinkman, E. A.; Berger, S.; Brauman, J. I. *J. Am. Chem. Soc.* **1994**, *116*, 8304−8310.
(67) Hwu, J. R.; Wong, F. F.; Huang, J.-J.; Tsay, S.-C. *J. Org. Chem.* **1997**, *62*, 4097−4104.
(68) Kabytaev, K. Z.; Everett, T. A.; Safronov, A. V.; Sevryugina, Y. V.; Jalisatgi, S. S.; Hawthorne, M. F. *Eur. J. Inorg. Chem.* **2013**, 2488−2491.
(69) Evans, D. R.; Reed, C. A. *J. Am. Chem. Soc.* **2000**, *122*, 4660−4667.
(70) Cheng, R. J.; Latos-Grazynski, L.; Balch, A. L. *Inorg. Chem.* **1982**, *21*, 2412−2418.
(71) Scheidt, W. R.; Reed, C. A. *Chem. Rev.* **1981**, *81*, 543−555.
(72) A short Fe−S distance of 2.177(1) Å was reported for a low-spin six-coordinate iron(III) alkanethiolate complex: See Suzuki, N.; Higuchi, T.; Urano, Y.; Kikuchi, K.; Uekusa, H.; Ohashi, Y.; Uchida, T.; Kitagawa, T.; Nagano, T. *J. Am. Chem. Soc.* **1999**, *121*, 11571−11572.
(73) Franke, A.; Hessenauer-Ilicheva, N.; Meyer, D.; Stochel, G.; Woggon, W.-D.; van Eldik, R. *J. Am. Chem. Soc.* **2006**, *128*, 13611−13624.
(74) Byrn, M. P.; Strouse, C. E. *J. Am. Chem. Soc.* **1981**, *103*, 2633−2635.
(75) Higuchi, T.; Uzu, S.; Hirobe, M. *J. Am. Chem. Soc.* **1990**, *112*, 7051−7053.
(76) Huang, Y.-P.; Kassner, R. J. *J. Am. Chem. Soc.* **1979**, *101*, 5807−5810.
(77) Jones, D. H.; Hinman, A. S. *Can. J. Chem.* **2000**, *78*, 1318−1324.
(78) Green, M. T. *J. Am. Chem. Soc.* **1999**, *121*, 7939−7940.
(79) Salinger, R. M.; West, R. *J. Organomet. Chem.* **1968**, *11*, 631−633.
(80) Swistak, C.; Mu, X. H.; Kadish, K. M. *Inorg. Chem.* **1987**, *26*, 4360−4366.
(81) Shirazi, A.; Barbush, M.; Ghosh, S.; Dixon, D. W. *Inorg. Chem.* **1985**, *24*, 2495−2502.
(82) Wyllie, G. R. A.; Scheidt, W. R. *Chem. Rev.* **2002**, *102*, 1067−1090.
(83) Franke, A.; Roncaroli, F.; van Eldik, R. *Eur. J. Inorg. Chem.* **2007**, 773−798.
(84) Anzai, K.; Hatano, K.; Lee, Y. J.; Scheidt, W. R. *Inorg. Chem.* **1981**, *20*, 2337−2339.
(85) Adler, A. D.; Longo, F. R.; Kampas, F.; Kim, J. *J. Inorg. Nucl. Chem.* **1970**, *32*, 2443−2445.
(86) Otsuka, T.; Ohya, T.; Sato, M. *Inorg. Chem.* **1984**, *23*, 1777−1779.
(87) Fleischer, E. B.; Srivastava, T. S. *J. Am. Chem. Soc.* **1969**, *91*, 2403−2405.
(88) *Crystal Clear*. Rigaku/MSC, Inc.; Rigaku Corporation, The Woodlands, TX, 2005.
(89) *ABSCOR*. Higashi; Rigaku Corporation, Tokyo, Japan, 1995.
(90) Sheldrick, G. M. *SHELXTL97: Program for Refinement of Crystal Structures*; University of Göttingen: Göttingen, Germany, 1997.
(91) Sheldrick, G. M. *Acta Crystallogr., Sect. A: Found. Crystallogr.* **2008**, *A64*, 112−122.